Assessing the Impact of DER on the Expansion of Low-Carbon Power Systems Under Deep Uncertainty

Pablo Apablaza[1], Sebastián Püschel-Løvengreen, Rodrigo Moreno[1,2], Sleiman Mhanna[3] and Pierluigi Mancarella[3,4]

***Abstract*—This paper studies the impact of distributed energy resources (DER) on economic displacements or delays of power system investments. We investigate how the operational flexibility from DER controllability can influence the integrated expansion of transmission and energy storage. Given the interplay of flexibility provision from different technologies, accurately representing uncertainties is essential to avoid over- or under-estimating the flexible operational capabilities of DER. To address this challenge, we propose a multi-stage stochastic expansion planning model that can optimise transmission and storage investments, as well as DER services against long-term uncertainties and detailed operational constraints. We employ a four-stage scenario tree to represent uncertainties and a Dantzig-Wolfe decomposition within a column generation approach to tackle computational challenges. Case studies performed on real Australian National Electricity Market (NEM) scenarios demonstrate that a deterministic model overestimates the capabilities of controllable DER to displace transmission investments, particularly in early stages. Conversely, the proposed stochastic model provides a more measured assessment, maintaining a steadier estimate of transmission displacement potential by controllable DER throughout various stages.**

***Index Terms*—Distributed Energy Resources, Investment Under Uncertainty, Low-Carbon Power System Planning, Stochastic Optimisation, Australian Power System.**

NOMENCLATURE

Parameters

$\boldsymbol{A}_n$	Matrix linking operational and investment decisions, node n
$c^{\text{fuel}}_{n,g}$	Fuel cost, node n, generator g [\$/MW]
$c^{\text{sup/sdn}}_{g}$	Startup/shutdown cost, generator g [\$]
$c^{\text{shup/shdn}}_{d}$	Cost of load shift up/down, DER d [\$/MW]
c^{red}_{d}	Cost of load reduction, DER d [\$/MW]
$\boldsymbol{c}^{\text{inv/op}}_{n}$	Vectors of investment/operational cost, node n
$D_{n,b,t}$	Demand, node n, bus b, time t [MW]
$\bar{E}_e, \underline{E}_e$	Max./min. energy capacity, ESS e [MWh]
$\bar{F}_{l,t}/\underline{F}_{l,t}$	Max. forward/reverse flow, line l, time t [MW]
$\mathcal{F}_g/\mathcal{P}_g$	Full/partial outage rate, generator g [%]
$\text{LL}_{n,a}$	Largest load loss, node n, area a [MW]
NT	Number of hours per representative period
$\text{N}_{n,g}$	Maximum number of online units, node n, gen. g
$\bar{P}_g/\underline{P}_g$	Max./min. power output, generator g [MW]
$\bar{P}^{\text{pr/sr}^+}_{g}$	Max. capacity providing PR/SR, gen. g [MW]
$\bar{P}^{\text{ch/dch}}_{e}$	Max. charging/discharging power, ESS e [MW]
$\bar{P}^{\text{pr}}_{e}$	Max. cap. for primary reserves, ESS e [MW]
$\tilde{P}^{\text{R}}_{n,r,t}$	Renewable output, node n, gen. r, time t [MW]
r	Financial discount rate
$\text{R}^{\text{up/down}}_{g}$	Up/downward ramp limit, generator g [MW]
RS_{g}	Primary reserve slope, generator g
$\text{T}^{\text{up/dn}}_{g}$	Min. up/down times, generator g [h]
$\text{T}^{\text{sup/sdn}}_{g}$	Startup/shutdown times, generator g [h]
$\text{T}^{\text{pr/sr}}$	Time for primary/secondary reserve provision [s]
$\text{T}^{\text{rec}}_{d}$	Re-balance time duration for load shift, DER d [h]
VoLL	Value of Lost Load [\$/MW]
y_n	Number of years from node n to root node
$\bar{z}^{\text{L/E}}_{n,\hat{l}/\hat{e}}$	Capacity for investment, node n, line $\hat{l}$ / BESS $\hat{e}$
$\bar{z}^{\text{D}}_{n,d}$	Installed units, node n, DER d
$\bar{\boldsymbol{Z}}_n$	Vector of max. total installed units, node n
α_g	Derating factor due to partial outage, gen. g
$\bar{\gamma}^{\text{shup/shdn}}_{d}$	Max. up/down load shifting capacity, DER d [MW]
$\bar{\gamma}^{\text{red}}_{d}$	Max. load reduction capacity, DER d [MW]
Δf^{db}	Freq. response deadband target deviation [Hz]
$\Delta f^{\text{qssf}^{-/+}}$	Target QSS frequency low/high events [Hz]
ζ_d	Payback effect penalisation, DER d [%]
$\eta^{\text{ch/dch}}_{e}$	Charging/discharging efficiency, ESS e [%]
$\tilde{\kappa}_{n,\tilde{d},t}$	Reference power, node n, DER $\tilde{d}$, time t [MW]
$\xi_{n,h,w}$	Cap. factor, node n, hydro gen. h, period w [%]
$\pi^{\text{L/E}}_{n,\hat{l}/\hat{e}}$	Investment cost, node n, line $\hat{l}$/ESS $\hat{e}$ [\$]
ρ_n	Probability of node n
σ_a	Load damping factor, area a [%/Hz]
ω_w	Weight over one year, representative period w

Variables and functions

$e^{\text{E}}_{n,e,t}$	State of charge, node n, ESS e, time t [MWh]
$e^{\text{sh/up/dn}}_{n,d,t}$	State shift/up/down, node n, DER d, time t [MWh]
$f_{n,l,t}$	Power flow, node n, line l, time t [MW]
$f^{\text{p/n}}_{n,l,t}$	Positive/negative slack, node n, line l, time t [MW]
$LS_{n,b,t}$	Load shedding, node n, bus b, time t [MW]
$n_{n,g,t}$	Online units, node n, generator g, time t
$p_{n,g,t}$	Power output, node n, generator g, time t [MW]
$p^{\text{c}}_{n,r,t}$	Power curtailment, node n, gen. r, time t [MW]
$p^{\text{dch/ch}}_{n,e,t}$	Dis/charging power, node n, ESS e, time t [MW]
$p^{s^{ty}}_{n,g/e,t}$	Power scheduled for reserve service s (pr/sr), type ty (up/down), node n, gen. g/ESS e, time t [MW]
$x^{\text{L}}_{n,\hat{l}}$	Integer variable for investment, node n, line $\hat{l}$
$x^{\text{E}}_{n,\hat{e}}$	Integer variable for investment, node n, ESS $\hat{e}$
$z^{\text{L}}_{n,l}$	Total installed units, node n, transmission line l
$z^{\text{E}}_{n,e}$	Total installed units, node n, ESS e
$\boldsymbol{X}^{\text{inv/op}}_{n}$	Vector of investment/operation variables, node n
$\boldsymbol{Z}_n$	Vector of total installed units, node n
$\gamma^{\text{shup/shdn}}_{n,d,t}$	Up/downward shift, node n, DER d, time t [MW]
$\gamma^{\text{red}}_{n,d,t}$	Load reduction, node n, DER d, time t [MW]

[1]Department of Electrical Engineering, University of Chile, Santiago, Chile.
[2]Instituto Sistemas Complejos de Ingeniería (ISCI), Santiago, Chile.
[3]Department of Electrical and Electronic Engineering, The University of Melbourne, Melbourne, Australia.
[4]School of Electrical and Electronic Engineering, The University of Manchester, Sackville Street, Manchester M13 9PL, UK.

$\delta^{\text{sdn/sup}}_{n,g,t}$ Shutdown/startup, node n, gen. g, time t [MW]
$\Delta p^{\text{g-loss}}_{n,a,t}$ Gen. contingency size, node n, area a, time t [MW]
$\lambda_{n,j}$ Binary variable to select column j in node n
$\mu_{n,e,t}$ State of operation, node n, ESS e, time t
$\boldsymbol{\mu}_n/\boldsymbol{\pi}_n$ Dual variables for DW decomposition, node n
$\nu_{n,g,t}$ Power-on status, node n, generator g, time t
$\Omega^{\text{s}}_{n,a,t^{ty}}$ Allocation of power for reserve service s (pr/sr), type ty (up/down), node n, area a, time t [MW]

Indices and sets

$a, b \in \mathcal{A}, \mathcal{B}$ Areas, buses in the system
$d, \tilde{d} \in \mathcal{D}, \mathcal{D}_b$ DER in the system, in bus b
$e \in \mathcal{E}$ ESS in the system
$\tilde{e}, \bar{e} \in \mathcal{E}_b, \mathcal{E}_a$ ESS in bus b, in area a
$\hat{e} \in \mathcal{E}^{\text{c}} \subset \mathcal{E}$ Candidate ESS
$g \in \mathcal{G}$ Synchronous generators in the system
$\tilde{g}, \bar{g} \in \mathcal{G}_b, \mathcal{G}_a$ Synchronous generators in bus b, in area a
$h \in \mathcal{G}^{\text{H}} \subset \mathcal{G}$ Hydro generators in the system
$j \in \mathcal{K}_n$ Indices of elements in $\mathcal{Z}_n$
$l \in \mathcal{L}$ Transmission lines in the system
$\tilde{l} \in \mathcal{L}^{\text{from}}_b, \mathcal{L}^{\text{to}}_b$ Transmission lines from, to bus b
$\hat{l} \in \mathcal{L}^{\text{c}} \subset \mathcal{L}$ Candidate transmission lines
$n \in \mathcal{N}$ Nodes in the scenario tree
$m \in \mathcal{P}_n$ Predecessor nodes of node n
$r, \tilde{r} \in \mathcal{R}, \mathcal{R}_b$ Variable renewable gen. in the system, bus b
$t \in \mathcal{T}_w$ Hours within a representative period w
$w \in \mathcal{W}_n$ Representative periods, node n
$\mathcal{X}_n$ Feasible operational decisions, node n
$\mathcal{Z}_n$ Feasible total installed units, node n

I. Introduction

In transitioning towards low-carbon power systems, distributed energy resources (DER) can play a prominent role in providing flexibility services and displacing network investments, particularly in transmission lines and energy storage. The ability of DER to reshape load patterns, mitigate congestion in transmission systems, reduce reliance on high-cost generation units, and facilitate the integration of variable renewable energy underscores its potential value. Nevertheless, it is crucial to understand the real-world implications and analyse the potential of DER in economically displacing transmission and energy storage investments [1], considering various operational modes (centrally controlled or decentralised), detailed models of system operation, and long-term uncertainties. Our hypothesis posits that deterministic and stylised models, which overlook multiple sources of uncertainty and operational details, can distort the capacity of DER to displace investments in system infrastructure, a pitfall to avoid, as this can lead to sub-optimal investment decisions [2].

Regarding system expansion planning, numerous studies have explored the impact of DER technologies on system investments from an economic perspective. For instance, demand response [3]–[5], electric vehicles [6], and distributed generation [7]–[9] have demonstrated positive outcomes, highlighting DER as a source of flexibility capable of displacing system investments and reducing the risk of having stranded assets. DER influence in energy markets was studied in [5], [10], presenting considerable operational savings depending on the market share and aggregation capacity. From a modelling standpoint, DER integration has been approached through deterministic [6], [11], robust [3], and two-stage stochastic [4], [5] frameworks to study the integration of different flexible technologies emerging on the demand side.

Regarding uncertainty representation, most industry-based deterministic models often overlook uncertainties [2], while academia has increased its focus on addressing these issues [12], [13]. In particular, by quantifying uncertainty through probabilities, stochastic models strike a better cost-risk balance, and to better capture the decision dynamics and facilitate anticipatory strategic investments, recent research has further explored multi-stage models [2], [14], [15]. However, prior works in this domain have yet to investigate the integration of DER in system planning as an active flexibility source within multi-stage investment frameworks while addressing uncertainties across multiple scenarios. Bridging this gap in power system planning is of utmost importance given the increasing penetration of DER in modern grids, the deployment of which is surrounded by uncertainty, impacting demand growth as well as the available demand-side flexibility and, consequently, the need for investments in utility-scale assets.

In this context, we present a multi-stage, stochastic expansion planning model. It optimises investments in transmission and energy storage and the operation of controllable DER services while considering long-term uncertainties. Due to its multi-stage nature, it integrates and captures the growing DER penetration and controllability along with other sources of uncertainty within multiple investment periods. As transmission system operators and planners do not influence decisions in distribution networks, investment in new DER is out of the scope of this work. The proposed framework also incorporates unit commitment and security constraints and spans representative weeks over several years. We employ a column generation algorithm within a Dantzig-Wolfe decomposition to handle the large-scale optimisation problem. We develop a set of case studies on the Australian power system, utilising real scenarios and system parameters from the system operator (AEMO). Through these, we determine the influence of DER controllability and uncertainty modelling in changing transmission and energy storage investment portfolios and the differences between employing deterministic and stochastic models for its valuation in expansion planning. Hence, the main contributions are:

1) Provide a stochastic power system expansion planning framework incorporating a model for flexible technologies (DER), accounting for demand response and distributed storage as virtual power plants (VPP), and its operating modes (controllable and non-controllable) within a detailed system operation under uncertainty.

2) Analyse the impact of DER and its operating modes on displacing system investments over time and across multiple scenarios from a techno-economic point of view, showing the need to account for a detailed uncertainty representation in expansion planning to adequately value DER.

3) Assess how the choice of the modelling setting, whether multi-stage stochastic or deterministic, impacts the robustness

of investment portfolios when incorporating DER controllability across multiple scenarios.

The remainder of this paper is structured as follows. Section II presents the multi-stage stochastic expansion planning model. Section III delves into the system data utilised and the case studies considered. Section IV presents the results and discussion. Section V concludes.

II. The Stochastic Power System Expansion Planning Model

This section presents the multi-stage stochastic expansion planning model, expanding [2], [16] by including an operational model for DER through aggregators. The model minimises the expected investment and operational costs and allows managing (i) long-term uncertainty through a multi-stage scenario tree, associated with investment costs, fuel prices, installed capacity of variable renewable energy (VRE), DER and energy storage, the retirement of coal units and load growth. (ii) detailed short-term operational constraints (unit commitment, reserves to manage short-term uncertainty, storage and DER flexibility services) related to the capacity of technologies to cope with VRE outputs and demand.

A. Multi-stage scenario tree approach

The expansion planning model is formulated as a multi-stage stochastic problem to account for long-term uncertainties. These uncertainties, associated with different parameters (investment costs, fuel prices, installed VRE, DER and energy storage, the retirement of coal units and load growth) are modelled using a scenario tree with $|\mathcal{S}|$ decision stages and $|\mathcal{N}|$ nodes. The root node (i.e. $n = 1$) represents the initial state of the system. Nodes n in each stage s represent potential states of the uncertain parameters within that stage. A node consists of an operational and an investment phase. Investments for the current node and its successors (child nodes) are determined within the investment phase, taking into account the lead times of candidate technologies.

For technologies with lead times (e.g. transmission lines), the investment decisions are made in each node n of the scenario tree prior to the disclosure of uncertain parameters in the subsequent stage. This ensures the new infrastructure is feasible under multiple stochastically modelled scenarios. This seeks to represent the reality of the infrastructure planning problem, where here-and-now and wait-and-see decisions for large-scale assets are made under the uncertainty of the future that the system could face. Subsequently, the operation of the system at each node n employs the existing and new infrastructure to meet different operational requirements.

B. Mathematical formulation

1) Objective function: shown in (1), aims to minimise the discounted expected value of the total cost. The expected total cost includes the investment and operational costs of every node n of the scenario tree. The investment cost for each node (2) is calculated by summing up the annuities paid for new transmission and storage assets if the decision is made to invest in them. The operational cost of the system (3) is given by the operation of a set of representative weeks $\mathcal{W}_n$ for each node n. The operational cost includes costs for fuel, start-up and shut-down of synchronous units, controllable DER services (load shifting and reduction), and load shedding.

$$\min_{\boldsymbol{X}_n^{\text{inv}}, \boldsymbol{X}_n^{\text{op}}} \sum_{n\in\mathcal{N}} \frac{\rho_n}{(1+r)^{y_n}} \Big(C_n^{\text{inv}}\big(\boldsymbol{X}_n^{\text{inv}}\big) + C_n^{\text{op}}\big(\boldsymbol{X}_n^{\text{op}}\big) \Big) \tag{1}$$

$$C_n^{\text{inv}}(\boldsymbol{X}_n^{\text{inv}}) = \sum_{\hat{l}\in\mathcal{L}^{\text{c}}} \pi^{\text{L}}_{n,\hat{l}}(x^{\text{L}}_{n,\hat{l}} + z^{\text{L}}_{n,\hat{l}}) + \sum_{\hat{e}\in\mathcal{E}^{\text{c}}} \pi^{\text{E}}_{n,\hat{e}} z^{\text{E}}_{n,\hat{e}} \tag{2}$$

$$\begin{aligned} C_n^{\text{op}}(\boldsymbol{X}_n^{\text{op}}) = \sum_{b\in\mathcal{B}} \sum_{w\in\mathcal{W}_n} \sum_{t\in\mathcal{T}_w} \omega_w \Big(\sum_{\tilde{g}\in\mathcal{G}_b} \Big(c^{\text{fuel}}_{n,\tilde{g}} p_{n,\tilde{g},t} \\ + c^{\text{sup}}_{\tilde{g}} \delta^{\text{sup}}_{n,\tilde{g},t} + c^{\text{sdn}}_{\tilde{g}} \delta^{\text{sdn}}_{n,\tilde{g},t} \Big) + \sum_{\tilde{d}\in\mathcal{D}_b} \Big(c^{\text{shup}}_{\tilde{d}} \gamma^{\text{shup}}_{n,\tilde{d},t} + c^{\text{shdn}}_{\tilde{d}} \gamma^{\text{shdn}}_{n,\tilde{d},t} \\ + c^{\text{red}}_{\tilde{d}} \gamma^{\text{red}}_{n,\tilde{d},t} \Big) + \text{VoLL} \cdot LS_{n,b,t} \Big) \end{aligned} \tag{3}$$

2) Investment constraints: the construction of new assets is modelled through non-anticipativity constraints (4)-(5) [17]. These constraints guarantee that an investment made at a certain node n in the scenario tree is irreversible and will be available in the subsequent nodes connected to said node (child nodes). These also limit the number of new units installed in each node. For transmission lines, we consider a lead time of one stage between the investment decision ($x^{\text{L}}_{n,\hat{l}}$) and the availability of the asset ($z^{\text{L}}_{n,\hat{l}}$). Thus, new lines cannot be installed in the first investment stage (root node, $n = 1$) as imposed in (6). This condition is not imposed for BESS. We assume that BESS can be installed without a lead time (within the same stage), reflecting the reality and a key benefit of this technology. To represent real candidate projects, investment variables are binary for transmission lines and integer for BESS, as shown in (7)-(8).

$$z^{\text{L}}_{n,\hat{l}} \le \sum_{m\in\mathcal{P}_n} x^{\text{L}}_{m,\hat{l}} \le \bar{z}^{\text{L}}_{n,\hat{l}} \qquad \forall n, \hat{l} \tag{4}$$

$$z^{\text{E}}_{n,\hat{e}} \le \sum_{m\in\mathcal{P}_n} x^{\text{E}}_{m,\hat{e}} \le \bar{z}^{\text{E}}_{n,\hat{e}} \qquad \forall n, \hat{e} \tag{5}$$

$$z^{\text{L}}_{1,\hat{l}} = 0 \qquad \forall \hat{l} \tag{6}$$

$$x^{\text{L}}_{n,\hat{l}}, z^{\text{L}}_{n,\hat{l}} \in \{0,1\} \qquad \forall n, \hat{l} \tag{7}$$

$$x^{\text{E}}_{n,\hat{e}}, z^{\text{E}}_{n,\hat{e}} \in \mathbb{Z} \qquad \forall n, \hat{e} \tag{8}$$

3) Power system constraints: equations model power balance, reserves, power flow, transmission and generation limits and storage operation. Equation (9) ensures the power balance for the demand in every bus b at every hour t, for each representative period w and node n. The term $\tilde{\kappa}_{n,\tilde{d},t}$ models the reference power exchanges of non-controllable DER, which can be controlled by means of the available flexibility services they are able to provide.

$$\begin{aligned} \sum_{\tilde{g}\in\mathcal{G}_b\cup\mathcal{R}_b} p_{n,\tilde{g},t} + \sum_{\tilde{l}\in\mathcal{L}^{\text{to}}_b} f_{n,\tilde{l},t} - \sum_{\tilde{l}\in\mathcal{L}^{\text{from}}_b} f_{n,\tilde{l},t} + \sum_{\tilde{e}\in\mathcal{E}_b} \Big(p^{\text{dch}}_{n,\tilde{e},t} - p^{\text{ch}}_{n,\tilde{e},t} \Big) \\ = D_{n,b,t} - LS_{n,b,t} + \sum_{\tilde{d}\in\mathcal{D}_b} \tilde{\kappa}_{n,\tilde{d},t} + \sum_{\tilde{d}\in\mathcal{D}_b} \gamma^{\text{shup}}_{n,\tilde{d},t} \\ - \sum_{\tilde{d}\in\mathcal{D}_b} \gamma^{\text{shdn}}_{n,\tilde{d},t} - \sum_{\tilde{d}\in\mathcal{D}_b} \gamma^{\text{red}}_{n,\tilde{d},t}, \qquad \forall n, b, w, t \end{aligned} \tag{9}$$

Each synchronous unit (including hydro) is modelled through (10)-(14). Units are capable of providing primary (pr) and secondary (sr) reserves during high- and low-frequency events. Downward (-) reserves are described by (10). Upward (+) reserves are described by (11)-(13). Equation (14)

accounts for maximum generation, considering outage rates. The balance for each renewable generator is presented in (15), ensuring the available renewable resource at time t is balanced between injections and the curtailed power $p^{\mathrm{c}}_{n,r,t}$. Maximum run-of-river generation, based on historical inflow data, is presented in equation (16), while hydro unit capacity factors constrain energy generation from reservoirs (17).

$$n_{n,g,t}\underline{P}_g \leq p_{n,g,t} - p^{\mathrm{pr}^-}_{n,g,t} - p^{\mathrm{sr}^-}_{n,g,t} \quad \forall n,g,t \ (10)$$

$$p_{n,g,t} + \frac{p^{\mathrm{pr}^+}_{n,g,t}}{\mathrm{RS}_g} + p^{\mathrm{sr}^+}_{n,g,t} \leq n_{n,g,t}\bar{P}_g \quad \forall n,g,t \ (11)$$

$$p^{\mathrm{pr}^+}_{n,g,t} \leq n_{n,g,t}\bar{P}^{\mathrm{pr}^+}_g \quad \forall n,g,t \ (12)$$

$$p^{\mathrm{sr}^+}_{n,g,t} \leq n_{n,g,t}\bar{P}^{\mathrm{sr}^+}_g \quad \forall n,g,t \ (13)$$

$$p_{n,g,t} \leq n_{n,g,t}\cdot\bar{P}_g\left(1-(\mathcal{F}_g+\mathcal{P}_g(1-\alpha_g))\right) \quad \forall n,g,t \ (14)$$

$$p_{n,r,t} + p^{\mathrm{c}}_{n,r,t} = \tilde{P}^{\mathrm{R}}_{n,r,t} \quad \forall n,r,t \ (15)$$

$$p_{n,h,t} \leq \bar{P}_h \cdot n_{n,h,t}\cdot\xi_{n,h,w} \quad \forall n,h,t,w \ (16)$$

$$\textstyle\sum_{t\in\mathcal{T}_\omega} p_{n,h,t} \leq \mathrm{NT}\cdot\bar{P}_h\cdot n_{n,h,t}\cdot\xi_{n,h,w} \quad \forall n,h,t,w \ (17)$$

The operation of storage technologies, as BESS, pumped (PSS), and VPP, is described in equations (18)-(27). Integer variable $\mu_{n,e,t}$ is used to determine in (18) and (19) the power injection or consumption, while (20) limits the charging and discharging power. Upward and downward reserves are modelled through (21) and (22). The maximum level of primary reserves (pr) is set through (23). The energy balance is described in (24) and (25). Equations (26) and (27) guarantee the storage has the capacity to provide reserves for the time required in each service. VPP are not providing reserves.

$$p^{\mathrm{ch}}_{n,e,t} \leq \left(1-\mu_{n,e,t}\right)\cdot\bar{P}^{\mathrm{ch}}_e \quad \forall n,e,t \ (18)$$

$$p^{\mathrm{dch}}_{n,e,t} \leq \mu_{n,e,t}\cdot\bar{P}^{\mathrm{dch}}_e \quad \forall n,e,t \ (19)$$

$$p^{\mathrm{ch/dch}}_{n,e,t} \leq \bar{P}^{\mathrm{ch/dch}}_e z^{\mathrm{E}}_{n,e} \quad \forall n,e,t \ (20)$$

$$p^{\mathrm{pr}^+}_{n,e,t} + p^{\mathrm{sr}^+}_{n,e,t} \leq \mu_{n,e,t}\bar{P}^{\mathrm{dch}}_e - p^{\mathrm{dch}}_{n,e,t} + p^{\mathrm{ch}}_{n,e,t} \quad \forall n,e,t \ (21)$$

$$p^{\mathrm{pr}^-}_{n,e,t} + p^{\mathrm{sr}^-}_{n,e,t} \leq \left(1-\mu_{n,e,t}\right)\bar{P}^{\mathrm{ch}}_e + p^{\mathrm{dch}}_{n,e,t} - p^{\mathrm{ch}}_{n,e,t} \forall n,e,t \ (22)$$

$$p^{\mathrm{pr}^-}_{n,e,t}, p^{\mathrm{pr}^+}_{n,e,t} \leq \bar{P}^{\mathrm{pr}}_e \quad \forall n,e,t \ (23)$$

$$e^{\mathrm{E}}_{n,e,t} = \eta^{\mathrm{ch}}_e p^{\mathrm{ch}}_{n,e,t} - \frac{p^{\mathrm{dch}}_{n,e,t}}{\eta^{\mathrm{dch}}_e} + e^{\mathrm{E}}_{n,e,t-1} \quad \forall n,e,t:t>1 \ (24)$$

$$\underline{E}_e z^{\mathrm{E}}_{n,e} \leq e^{\mathrm{E}}_{n,e,t} \leq \bar{E}_e z^{\mathrm{E}}_{n,e} \quad \forall n,e,t \ (25)$$

$$p^{\mathrm{pr}^+}_{n,e,t}\mathrm{T}^{\mathrm{pr}} + p^{\mathrm{sr}^+}_{n,e,t}\mathrm{T}^{\mathrm{sr}} \leq e^{\mathrm{E}}_{n,e,t} - \underline{E}_e \quad \forall n,e,t \ (26)$$

$$p^{\mathrm{pr}^-}_{n,e,t}\mathrm{T}^{\mathrm{pr}} + p^{\mathrm{sr}^-}_{n,e,t}\mathrm{T}^{\mathrm{sr}} \leq \bar{E}_e - e^{\mathrm{E}}_{n,e,t} \quad \forall n,e,t \ (27)$$

Forward and reverse maximum capacity of transmission lines are modelled as presented in (28). Equations (29)-(30) use slack variables $f^{\mathrm{p}}_{n,l,t}$, $f^{\mathrm{n}}_{n,l,t}$ to define the transmission head room in each direction.

$$-\underline{F}_{l,t}z^{\mathrm{L}}_{n,l} \leq f_{n,l,t} \leq \bar{F}_{l,t}z^{\mathrm{L}}_{n,l} \quad \forall n,l,t \ (28)$$

$$f_{n,l,t} + f^{\mathrm{p}}_{n,l,t} = \bar{F}_{l,t}z^{\mathrm{L}}_{n,l} \quad \forall n,l,t \ (29)$$

$$f_{n,l,t} + f^{\mathrm{n}}_{n,l,t} = -\underline{F}_{l,t}z^{\mathrm{L}}_{n,l} \quad \forall n,l,t \ (30)$$

Equations (31)-(32) describe the total allocation of power for primary and secondary reserves of type ty in each area a and time t. Equation (33) determines the size of the contingency for the largest loss of generation in each area a of the system. The quasi-steady state frequency (QSSF) constraints [16] are modelled through (35)-(38), ensuring the availability of primary and secondary upward and downward reserves in the system to restore the QSSF in the case of the biggest possible loss of generation or load in each area a.

$$\Omega^{\mathrm{pr}^{ty}}_{n,a,t} = \textstyle\sum_{\bar{g}\in\mathcal{G}_a} p^{\mathrm{pr}^{ty}}_{n,\bar{g},t} + \sum_{\bar{e}\in\mathcal{E}_a} p^{\mathrm{pr}^{ty}}_{n,\bar{e},t} \quad \forall n,a,t,ty \ (31)$$

$$\Omega^{\mathrm{sr}^{ty}}_{n,a,t} = \textstyle\sum_{\bar{g}\in\mathcal{G}_a} p^{\mathrm{sr}^{ty}}_{n,\bar{g},t} + \sum_{\bar{e}\in\mathcal{E}_a} p^{\mathrm{sr}^{ty}}_{n,\bar{e},t} \quad \forall n,a,t,ty \ (32)$$

$$\Delta p^{\text{g-loss}}_{n,a,t} \geq p_{n,\bar{g},t} \quad \forall n,a,\bar{g},t \ (33)$$

$$\bar{D}_{n,a,t} = D_{n,a,t} - \mathrm{LL}_{n,a} \quad \forall n,a,t \ (34)$$

$$\Omega^{\mathrm{pr}^+}_{n,a,t} \geq \Delta p^{\text{g-loss}}_{n,a,t} + \sigma_a D_{n,a,t}\Delta f^{\mathrm{qssf}^-} \quad \forall n,a,t \ (35)$$

$$\Omega^{\mathrm{pr}^-}_{n,a,t} \geq \mathrm{LL}_{n,a} - \sigma_a \bar{D}_{n,a,t}\Delta f^{\mathrm{qssf}^+} \quad \forall n,a,t \ (36)$$

$$\Omega^{\mathrm{sr}^+}_{n,a,t} \geq \Delta p^{\text{g-loss}}_{n,a,t} - \sigma_a D_{n,a,t}\left|\Delta f^{\mathrm{db}}\right| \quad \forall n,a,t \ (37)$$

$$\Omega^{\mathrm{sr}^-}_{n,a,t} \geq \mathrm{LL}_{n,a} - \sigma_a \bar{D}_{n,a,t}\left|\Delta f^{\mathrm{db}}\right| \quad \forall n,a,t \ (38)$$

4) Unit-commitment (UC) constraints: these model the unit scheduling, ramp limitations, startup/shutdown requirements, and minimum on-off times of conventional generators [18]. The online unit count and transitions are detailed in (39), with minimum up- and down-times $\mathrm{T}^{\mathrm{up}}_g$, $\mathrm{T}^{\mathrm{dn}}_g$ modelled through (40) and (41), respectively. Also, (41) integrates transition times $\mathrm{T}^{\mathrm{sup}}_g$, $\mathrm{T}^{\mathrm{sdn}}_g$ for unit startup and shutdown. The change of each unit g output between periods adheres to ramping ability and unit activation patterns in (42). The maximum downward change is determined by unit ramping and shutdowns in (43). Equations (44)-(45) restrict the number of committed units. For large generation clusters, integer variables $\nu_{n,g,t}$, $n_{g,t}$, $\delta^{\mathrm{sup}}_{g,t}$ and $\delta^{\mathrm{sdn}}_{g,t}$ can be relaxed without significant errors [18].

$$n_{n,g,t} - n_{n,g,t-1} = \delta^{\mathrm{sup}}_{n,g,t} - \delta^{\mathrm{sdn}}_{n,g,t} \quad \forall n,g,t>1 \ (39)$$

$$n_{n,g,t} \geq \textstyle\sum_{\tau=t-\mathrm{T}^{\mathrm{up}}_g}^{t} \delta^{\mathrm{sup}}_{n,g,\tau} \quad \forall n,g,t \ (40)$$

$$n_{n,g,t} \leq \mathrm{N}_{n,g} - \textstyle\sum_{\tau=t-\mathrm{T}^{\mathrm{sdn}}_g-\mathrm{T}^{\mathrm{sup}}_g-\mathrm{T}^{\mathrm{dn}}_g}^{t} \delta^{\mathrm{sdn}}_{n,g,\tau} \quad \forall n,g,t \ (41)$$

$$p_{n,g,t} - p_{n,g,t-1} \leq n_{n,g,t-1}\cdot\mathrm{R}^{\mathrm{up}}_g + \delta^{\mathrm{sup}}_{g,t}\cdot\underline{P}_g \quad \forall n,g,t \ (42)$$

$$p_{n,g,t-1} - p_{n,g,t} \leq n_{n,g,t-1}\cdot\mathrm{R}^{\mathrm{down}}_g + \delta^{\mathrm{sdn}}_{n,g,t}\cdot\underline{P}_g \quad \forall n,g,t \ (43)$$

$$\delta^{\mathrm{sup}}_{n,g,t} - \delta^{\mathrm{sdn}}_{n,g,t} \leq \mathrm{N}_{n,g}\cdot\nu_{n,g,t} \quad \forall n,g,t \ (44)$$

$$n_{n,g,t} \leq \mathrm{N}_{n,g}\cdot\nu_{n,g,t} \quad \forall n,g,t \ (45)$$

5) Controllable DER constraints: distributed energy resources can offer various flexibility services through its controllability, outlined in (46)-(51). Equations (46)-(48) model the load shifting, where the shifted load is re-balanced at intervals of $\mathrm{T}^{\mathrm{rec}}_d$ periods. Load shifting accounts for the payback effect, parameterised by ζ_d, reflecting the interaction between physical characteristics of different appliances (loads that can be shifted) [19]. DER are capable of providing these flexibility services (load shifting and load reduction/peak shaving) in each bus b of the system, which are aggregated in the balance equation (9) and limited through (49)-(51).

$$e^{\mathrm{sh}}_{n,d,t} = \gamma^{\mathrm{shdn}}_{n,d,t}\cdot(1+\zeta_d) - \gamma^{\mathrm{shup}}_{n,d,t} + e^{\mathrm{sh}}_{n,d,t-1} \quad \forall n,d,t \ (46)$$

$$e^{\mathrm{shup}}_{n,d,t} = (1+\zeta_d)\cdot e^{\mathrm{shdn}}_{n,d,t} \quad \forall n,d,t:t \bmod \mathrm{T}^{\mathrm{rec}}_d = 0 \ (47)$$

$$e^{\mathrm{shup/shdn}}_{n,d,t} = e^{\mathrm{shup/shdn}}_{n,d,t-1} + \gamma^{\mathrm{shup/shdn}}_{n,d,t} \quad \forall n,d,t:t>1 \ (48)$$

$$0 \leq \gamma^{\text{shup}}_{n,d,t} \leq \bar{\gamma}^{\text{shup}}_{d}\, \bar{z}^{\text{D}}_{n,d} \qquad \forall n,d,t \quad (49)$$

$$0 \leq \gamma^{\text{shdn}}_{n,d,t} \leq \bar{\gamma}^{\text{shdn}}_{d}\, \bar{z}^{\text{D}}_{n,d} \qquad \forall n,d,t \quad (50)$$

$$0 \leq \gamma^{\text{red}}_{n,d,t} \leq \bar{\gamma}^{\text{red}}_{d}\, \bar{z}^{\text{D}}_{n,d} \qquad \forall n,d,t \quad (51)$$

C. Solution methodology: Dantzig-Wolfe decomposition and column generation algorithm

The proposed model is a complex Mixed-Integer Linear Problem (MILP), which presents execution time and memory challenges for large systems. To address this, prior research [15] has explored techniques like the Dantzig-Wolfe (DW) decomposition. This effectively handles computational burden and allows obtaining an integer feasible solution for every investment stage [17] by breaking down the problem into independent subproblems. We reformulate the problem using the approach outlined in [17]. It defines a feasible region $\mathcal{Z}_n$ for total installed units in each node n. This region is expressed as a combination of a finite set of integer points $\{\hat{\boldsymbol{Z}}_{n,j}\}_{j\in\mathcal{K}_n}$ in $\mathcal{Z}_n$. For each feasible vector of installed units $\hat{\boldsymbol{Z}}_{n,j}$, there exists an optimal operational plan $\hat{\boldsymbol{X}}^{\text{op}}_{n,j}$. This allows $\boldsymbol{X}^{\text{op}}_{n}$ to be expressed as a convex combination of different plans $\hat{\boldsymbol{X}}^{\text{op}}_{n,j}$.

$$\mathcal{Z}_n = \{\boldsymbol{Z}_n \in \mathbb{Z}^+ | \exists \boldsymbol{X}^{\text{op}}_n \in \mathcal{X}_n,\ \boldsymbol{A}_n\boldsymbol{X}^{\text{op}}_n \leq \boldsymbol{Z}_n \leq \bar{\boldsymbol{Z}}_n\} \quad (52)$$

$$\boldsymbol{Z}_n = \textstyle\sum_{j\in\mathcal{K}_n} \lambda_{n,j}\hat{\boldsymbol{Z}}_{n,j}, \sum_{j\in\mathcal{K}_n} \lambda_{n,j} = 1, \lambda_{n,j} \in \{0,1\} \quad (53)$$

$$\boldsymbol{X}^{\text{op}}_n = \textstyle\sum_{j\in\mathcal{K}_n} \lambda_{n,j}\hat{\boldsymbol{X}}^{\text{op}}_{n,j} \quad (54)$$

$$\min \textstyle\sum_{n\in\mathcal{N}} \rho_n \left(\boldsymbol{c}^{\text{inv}\top}_n \boldsymbol{X}^{\text{inv}}_n + \sum_{j\in\mathcal{K}_n} \lambda_{n,j}\boldsymbol{c}^{\text{op}\top}_n \hat{\boldsymbol{X}}_{n,j}\right) \quad (55)$$

$$\text{s.t.:}\ \textstyle\sum_{j\in\mathcal{K}_n} \lambda_{n,j}\hat{\boldsymbol{Z}}_{n,j} \leq \sum_{h\in\mathcal{P}_n} \boldsymbol{X}^{\text{inv}}_h \qquad [\boldsymbol{\pi}_n] \quad (56)$$

$$\textstyle\sum_{j\in\mathcal{K}_n} \lambda_{n,j} = 1, \quad \lambda_{n,j} \in \{0,1\} \qquad [\boldsymbol{\mu}_n] \quad (57)$$

$$\boldsymbol{X}^{\text{inv}}_n \in \mathbb{Z}^+ \quad (58)$$

$$(\text{SP})_n \quad z^{\text{sp}}_n = \min\ \rho_n \boldsymbol{c}^{\text{op}\top}_n \boldsymbol{X}^{\text{op}}_n - \boldsymbol{\pi}^{\top}_n \boldsymbol{Z}_n - \boldsymbol{\mu}_n \quad (59)$$

$$\text{s.t.:}\quad \boldsymbol{X}^{\text{op}}_n \in \mathcal{X}_n \quad (60)$$

$$\boldsymbol{A}_n\boldsymbol{X}^{\text{op}}_n \leq \boldsymbol{Z}_n \leq \bar{\boldsymbol{Z}}_n,\ \ \boldsymbol{Z}_n \in \mathbb{Z}^+ \quad (61)$$

The master problem (55)-(58) is reformulated by substituting $\boldsymbol{Z}_n$ and $\boldsymbol{X}^{\text{op}}_n$ in the original formulation. Constraints (56)-(57) ensure the selection of one and only one vector of operation and investments. The associated dual prices of these constraints are $\boldsymbol{\pi}_n$ and $\boldsymbol{\mu}_n$. The master problem can be solved by using Column Generation, allowing obtaining columns $\{\hat{\boldsymbol{Z}}_{n,j}, \hat{\boldsymbol{X}}^{\text{op}}_{n,j}\}$ by solving subproblem $(\text{SP})_n$ for each node n of the scenario tree, which minimises the reduced cost of the generated column [17].

III. Case Study Applications

A. System characterisation and input data

Case study applications are based on the Australian NEM, which has been divided into ten sub-regions by the system operator for planning purposes, constituting the 10-bus system model presented in Fig. 1. It illustrates the topology, existing generation, transmission, storage, and expansion options. Key parameters of transmission candidates are outlined in Table I. Generation capacity, expected deployment of DER, retirement of coal units, existing storage and investment and fuel costs are obtained from the outcomes of ISP 2022 [20] for each scenario.

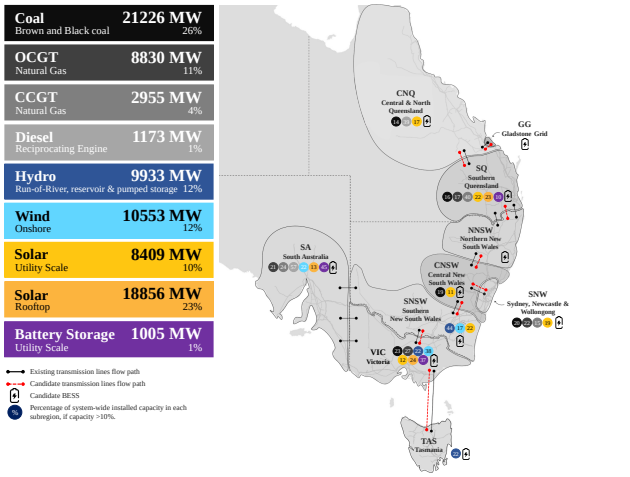

Fig. 1. Sub-regional topology of the National Electricity Market (NEM), Australia. Existing and candidate transmission line flow paths are in black and red, respectively. Circles contain the percentage of subregional installed capacity relative to the system total, categorised by technology.

A clustered unit commitment approach [18] reduces the number of generators to 59, comprising a total of 304 units. The parameters of generators are described in Table II for the year 2022 [20]. The VoLL in the NEM is 15,000 A$/MWh, and the discount rate is 10%. The QSSF target for a generator loss is 49.5 Hz, and the load damping factor is 2%. The system's largest single generation and load losses are 744 MW and 300 MW, respectively. For existing and candidate BESS, the round-trip efficiency is 81%, and for PSS is 70%.

TABLE I
RANGES OF PARAMETERS OF CANDIDATE TRANSMISSION LINES [20]

Reg. A	Reg. B	Nº options	Transfer limits [MW] A to B	Transfer limits [MW] B to A	Inv. Cost [$MM/MW]
CNQ	GG	1	550	500	0.74
SQ	CNQ	3	0 - 1500	300 - 1500	0.18 - 1.08
NNSW	SQ	3	550 - 1800	800 - 2000	0.48 - 1.56
CNSW	NNSW	11	585 - 2750	470 - 2750	0.18 - 2.72
CNSW	SNW	6	600 - 5000	0 - 5000	0.18 - 3.76
SNSW	CNSW	3	2000 - 2200	2000 - 2200	0.48 - 1.51
VIC	SNSW	5	1930 - 2000	1500 - 2000	1.16 - 1.52
TAS	VIC	2	750	750	1.87 - 3.17

TABLE II
TECHNO-ECONOMIC PARAMETERS OF SYNCHRONOUS GENERATORS [20]

Technology	Coal	Hydro	OCGT	CCGT	Diesel
Number of units	48	104	85	19	22
Variable cost [$/MWh]	13-30	7.5	117-181	64-100	127-478
Start-up costs [k$]	27-57	–	0.4-6.5	12-46	–
Rated power [MW]	280-744	15-144	33-219	48-385	31-114
Forced outage rate [pu]	0.76-0.86	0.97	0.93-0.94	0.95	0.93
MSG [MW]	110-330	3-29	11-72	20-190	6-22
Ramp rate [MW/min]	4-8	–	3-7	2-11	–
Min up time [h]	8-16	–	–	4-6	–

The controllable DER model assumes they actively participate in the market, while the non-controllable model is a behind-the-meter setting (fixed profiles). Distributed energy storage is represented as a VPP operated by an aggregator [20]. The demand response schema allows load shifting with

a maximum recovery time T_d^{rec} of 24 hours, with an additional 10% energy consumption payback. Reference capacities and durations of flexible technologies are outlined in Fig. 2. The DER trends for each scenario are illustrated in Fig. 3.

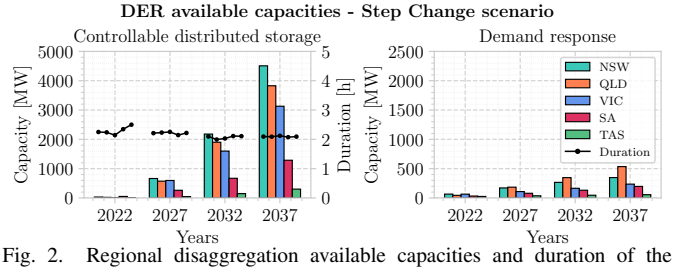

Fig. 2. Regional disaggregation available capacities and duration of the studied flexible DER technologies for AEMO's Step Change scenario [20].

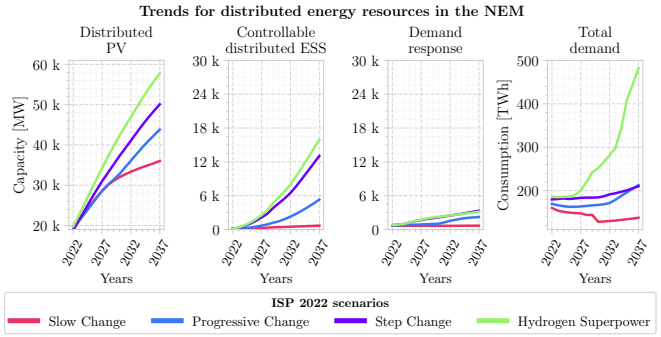

Fig. 3. 15-year forecast for distributed energy resources and total annual demand in AEMO's 2022 Integrated System Plan scenarios. Controllable distributed ESS corresponds to the capacity that is modelled as a VPP.

B. Multi-stage scenario tree

The multi-stage scenario tree employed in the problem formulation is displayed in Fig. 4. This tree is built upon the four scenarios devised by AEMO for their 2022 Integrated System Plan [20] and covers a horizon of 20 years through the 4 stages considered. AEMO has assigned probabilities of 4%, 29%, 50%, and 17% to these scenarios, encapsulating varying degrees of uncertainty across several critical parameters, including load growth, VRE, decommissioning of coal units, fuel and investment costs, and DER adoption (see Fig. 3). To refine the scenario tree and emulate transitions between scenarios [2], intermediate scenarios are created based on the information provided for the original scenarios, resulting in a total of 18 scenarios. The probabilities for the transition between nodes, ρ_n are determined by considering the number of child nodes for each node and the probabilities of the original scenarios.

C. Case Studies

The studies analyse four cases to illustrate and assess the impact of flexible technologies (VPP and demand response) in joint transmission and storage expansion planning.

We determine the optimal investments by solving the 4-stage stochastic optimisation model, following the scenario tree structure and the deterministic problems obtained from disaggregating the scenario tree into its individual scenarios, as outlined in Fig. 4. For each setting, we develop a case where flexible DER technologies can be centrally controlled (i.e. active market participants) and another when they are not able to be controlled (i.e. behind-the-meter model, without market interactions). The investment candidates for the four resulting cases are the ones described in Section III-A.

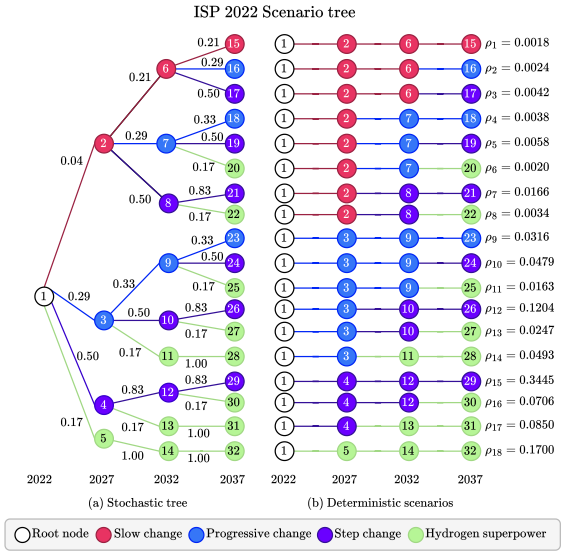

Fig. 4. (a) Multi-stage stochastic scenario tree and (b) deterministic scenarios for the 2022 AEMO Integrated System Plan. The stochastic tree in (a) has $|\mathcal{S}| = 4$ stages and $|\mathcal{N}| = 32$ nodes. This tree is disaggregated in (b) into 18 independent deterministic scenarios, each with a given probability ρ_s. For example, the deterministic scenario 15 has a probability $\rho_{15} = 0.3445$, which is obtained with the probability of each corresponding node that forms the scenario from the scenario tree (1, 4, 12, 29).

IV. Results and Discussion

In this section, we present and analyse the model's investment portfolios for additional transmission and energy storage under two main assumptions: (i) the modelling approach: deterministic and stochastic, and (ii) the ability of DER to provide operational flexibility (controllable / non-controllable). We solved each case of the stochastic approach employing the column generation algorithm outlined in section II-C, imposing a maximum tolerance for the MIP gap of 1% for each subproblem and master problem.

A. Impact of DER controllability on transmission investments

This section investigates the impact of flexible DER technologies on transmission investment portfolios and how the modelling framework employed assesses this flexibility. We modelled four stages and obtained the transmission investments. The investment results for both deterministic and stochastic models are summarised in Fig. 5. Each subfigure shows the probability of building a given aggregated transmission line capacity (i.e. the sum of the capacities of all lines built) in each investment stage.

When employing the deterministic approach, enabling DER controllability reduces expected installed transmission capacity by 38%, 9% and 5% in the respective investment years (2027, 2032 and 2037) when comparing the results scenario by scenario. Given these values and the corresponding probability distribution, it is important to note that to reduce transmission investments, this approach highly values the flexibility of controllable DER in the first stage of investment and considerably less in subsequent stages. This translates into a higher investment risk, as the deployment of a higher capacity of controllable DER is expected to occur in the long term than in the short term (as outlined in Fig. 3). In particular, the transmission infrastructure decided in 2022 (which becomes

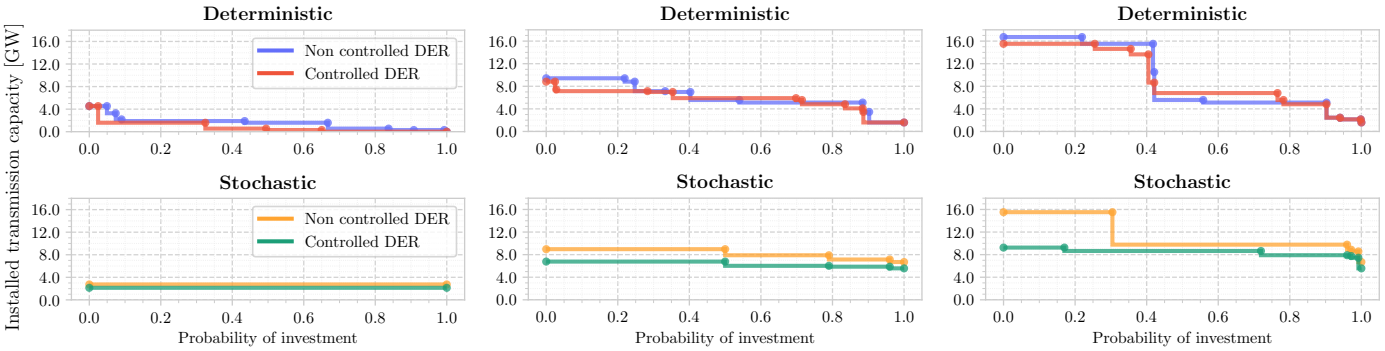

(a) Transmission investments 2027 (b) Transmission investments 2032 (c) Transmission investments 2037

Fig. 5. Transmission investment results for each stage and modelling approach.

available in 2027) has the risk of not being feasible in the range of all other scenarios in the subsequent stages.

Compared to the deterministic approach, the stochastic model shows an expected reduction of 22% of installed transmission capacity for 2027 and 23% for 2032 and 2037. This means that the model is more conservative in the first investment stage compared to the deterministic approach, and places a higher value on controllable DER to reduce transmission investments in later stages. These results showcase the advantages of the proposed stochastic model in capturing the growth of DER controllability, because the deployment is expected to be higher in the long than short term. In addition, the stochastic model shows that when DER controllability is not enabled, there is a probability of 30% of making a conservative decision to build significantly more transmission capacity, as indicated by the yellow curve in Fig. 7c. However, these investments are not made when DER are controllable, as seen in the green curve of Fig. 7c. Indeed, the stochastic model unlocks a risk-hedging value from the controllability of flexible technologies so that the investments that do not have a high probability are displaced, reducing the potential risk of having stranded assets.

B. Range of transmission expansion requirements

Fig. 6 shows the results corresponding to the minimum and maximum values of aggregated transmission capacity built. For example, regarding the minimum, in the year 2032 for the deterministic model, at least 1590 MW were built in the 18 scenarios. On the other hand, the maximum indicates the higher installed capacity in at least one of the scenarios (other scenarios build the same or less).

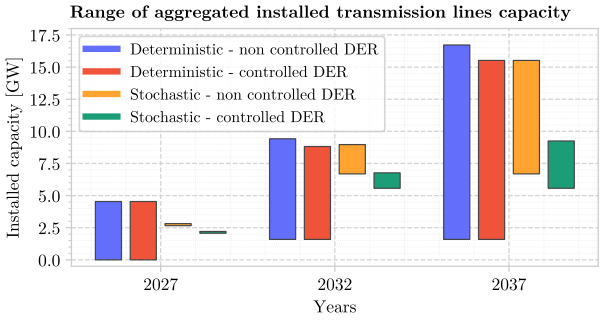

Fig. 6. Results for minimum and maximum requirements for expansion of capacity in transmission lines for each case.

The here-and-now decisions to build large-scale infrastructure that becomes available in 2027 are of crucial importance. When employing the deterministic model, the capacity that becomes available in that year varies from 0 to 4540 MW. This extensive array of future options indicates a low level of certainty regarding the required expansions across scenarios, leading to investments being undertaken with higher risks, even when controllable DER are enabled to actively participate in the market.

If we examine the year 2027 in the stochastic model with non-controllable DER, the investments are exactly 2740 MW, giving the planner a reliable answer about the anticipatory investments the system requires. Furthermore, when DER controllability is enabled, 2140 MW are installed. Thus, the stochastic model unlocks risk-hedging value from the controllable technologies to reduce 600 MW of transmission built while maintaining its ability to provide high certainty regarding the necessary expansions in the first stage.

Moreover, the path of investments resulting from employing the stochastic model presents higher robustness and anticipatory capabilities over time. This refers to the ability of the investment plan to perform well under a variety of different scenarios, reducing the planner's regret of having stranded assets in the face of potential overestimations. In particular, the case for the stochastic model with controllable DER presents the lowest difference between minimum and maximum built capacity across scenarios (as seen in the bar heights in Fig. 6). This result stems from the ability of the model to consider what benefits all scenarios, leading to a compromise solution. In contrast, deterministic practices yield portfolios tailored to specific scenarios, increasing the risk of investment inefficiencies.

C. The impact of DER on displacing storage investments

The objective of this section is to understand the interplay among the different sources that provide flexibility to the system (utility-scale, distributed storage and demand response) and how these interactions influence expansion decisions, particularly in a system that is transitioning to have a large number of flexible technologies. Fig. 7 shows the results of the stochastic model for built utility-scale storage (BESS).

In the studied cases, DER are expected to have an increased deployment towards the end of the period under analysis, as shown in Fig. 3. Based on the results, for the case of non-controlled DER, new BESS are deployed in the 3rd stage (2032), as shown in Fig. 7b. On the other hand, when the progressive integration of controllable DER is considered,

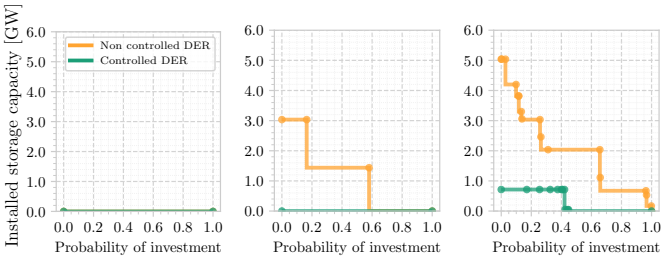

(a) 2027 (b) 2032 (c) 2037

Fig. 7. Probabilities of investment in utility-scale BESS for the stochastic model.

investments are delayed to the fourth stage (2037), as seen in Fig 7c. This is explained because the controllability of DER also allows for energy arbitrage purposes, therefore offering equivalent services to the grid. Thus, reducing the need for additional investments. Particularly, in the final stage new BESS are built in both cases, but with an expected reduction of 66% of installed capacity when controllability is enabled, thereby highlighting the impact of considering the deployment of controllable DER in saving costs in new energy storage investments.

V. Conclusions

This paper presented a comprehensive multi-stage framework for power system expansion planning under uncertainty with a model for controllable DER. We discussed four case studies within the Australian NEM, assessing and highlighting the potential and impact of DER in economically displacing network investments, including energy storage.

The results showed that selecting a stochastic mathematical framework is essential for progressively unlocking the risk-hedging value of controllable DER to define adequate system investment plans. In particular, the analysis shows that a deterministic model places a higher value on DER controllability for displacing network investments in the initial investment stage while neglecting the long-term flexibility that controllable DER could provide. In contrast, the proposed stochastic model steadily integrates the increasing controllability of DER into investment decisions made during all the stages, taking into account the higher DER penetration towards the end of the planning horizon. The analysis also shows that the stochastic model allows for narrowing down the investment candidates the planner should consider to build in the subsequent stages. Moreover, the range of built investment candidates is further narrowed down when controllable DER are enabled. Finally, the installation of utility-scale BESS is significantly reduced when enabling DER controllability, providing insight for policymakers to design incentives encouraging the deployment of DER for energy arbitrage purposes, and also highlighting the key role the coordination of distributed energy storage can play in future power systems serving as an alternative to utility-scale options.

Further research will delve deeper into the specific impact and valuation of controllable DER during extreme events. Additionally, employing risk metrics and a risk aversion analysis could help highlight the added value of operational flexibility offered by DER to manage constrained periods of system operation and the implications for expansion planning under uncertainty.

References

[1] I. J. Perez-Arriaga, "The Transmission of the Future: The Impact of Distributed Energy Resources on the Network," *IEEE Power and Energy Magazine*, vol. 14, no. 4, pp. 41–53, 7 2016.

[2] B. Moya, R. Moreno, S. Püschel-Løvengreen, A. M. Costa, and P. Mancarella, "Uncertainty representation in investment planning of low-carbon power systems," *Electric Power Systems Research*, vol. 212, 11 2022.

[3] D. Alvarado, A. Moreira, R. Moreno, and G. Strbac, "Transmission Network Investment with Distributed Energy Resources and Distributionally Robust Security," *IEEE Transactions on Power Systems*, vol. 34, no. 6, pp. 5157–5168, 11 2019.

[4] A. Inzunza, R. Moreno, A. Bernales, and H. Rudnick, "CVaR constrained planning of renewable generation with consideration of system inertial response, reserve services and demand participation," *Energy Economics*, vol. 59, pp. 104–117, 9 2016.

[5] T. Möbius, I. Riepin, F. Müsgens, and A. H. van der Weijde, "Risk aversion and flexibility options in electricity markets," *Energy Economics*, vol. 126, p. 106767, 10 2023.

[6] F. Manríquez, E. Sauma, J. Aguado, S. de la Torre, and J. Contreras, "The impact of electric vehicle charging schemes in power system expansion planning," *Applied Energy*, vol. 262, 3 2020.

[7] N. Matute, S. Torres, and C. Castro, "Transmission Expansion Planning Considering the Impact of Distributed Generation," in *ISGT - Europe*, Bucharest, 2019.

[8] P. Vilaça Gomes and J. Tome Saraiva, "Transmission System Planning Considering Solar Distributed Generation Penetration," in *International Conference on European Electricity Market, EEM*, 2017.

[9] F. Luo, J. Zhao, J. Qiu, J. Foster, Y. Peng, and Z. Dong, "Assessing the transmission expansion cost with distributed generation: An australian case study," *IEEE Transactions on Smart Grid*, vol. 5, no. 4, pp. 1892–1904, 2014.

[10] D. Papadaskalopoulos, G. Strbac, P. Mancarella, M. Aunedi, and V. Stanojevic, "Decentralized participation of flexible demand in electricity markets - Part II: Application with electric vehicles and heat pump systems," *IEEE Transactions on Power Systems*, vol. 28, no. 4, pp. 3667–3674, 2013.

[11] E. F. Alvarez, L. Olmos, A. Ramos, K. Antoniadou-Plytaria, D. Steen, and L. A. Tuan, "Values and impacts of incorporating local flexibility services in transmission expansion planning," *Electric Power Systems Research*, vol. 212, 11 2022.

[12] P. Mancarella, S. Püschel-Løvengreen, L. Zhang, and C. B. Domenech, "Study of advanced modelling for network planning under uncertainty. Part 1: Review of frameworks and industrial practices for decision-making in transmission network planning," 2020.

[13] L. A. Roald, D. Pozo, A. Papavasiliou, D. K. Molzahn, J. Kazempour, and A. Conejo, "Power systems optimization under uncertainty: A review of methods and applications," *Electric Power Systems Research*, vol. 214, 1 2023.

[14] R. Moreno, A. Street, J. M. Arroyo, and P. Mancarella, "Planning low-carbon electricity systems under uncertainty considering operational flexibility and smart grid technologies," *Philosophical Transactions of the Royal Society A: Mathematical, Physical and Engineering Sciences*, vol. 375, no. 2100, 8 2017.

[15] A. Flores-Quiroz and K. Strunz, "A distributed computing framework for multi-stage stochastic planning of renewable power systems with energy storage as flexibility option," *Applied Energy*, vol. 291, 6 2021.

[16] S. Püschel-Løvengreen, M. Ghazavi Dozein, S. Low, and P. Mancarella, "Separation event-constrained optimal power flow to enhance resilience in low-inertia power systems," *Electric Power Systems Research*, vol. 189, 12 2020.

[17] K. J. Singh, A. B. Philpott, and R. K. Wood, "Dantzig-Wolfe Decomposition for Solving Multistage Stochastic Capacity-Planning Problems," *Operations Research*, vol. 57, no. 5, pp. 1271–1286, 2009.

[18] L. Zhang, T. Capuder, and P. Mancarella, "Unified Unit Commitment Formulation and Fast Multi-Service LP Model for Flexibility Evaluation in Sustainable Power Systems," *IEEE Transactions on Sustainable Energy*, vol. 7, no. 2, pp. 658–671, 4 2016.

[19] J. A. Schachter and P. Mancarella, "Demand Response Contracts as Real Options: A Probabilistic Evaluation Framework under Short-Term and Long-Term Uncertainties," *IEEE Transactions on Smart Grid*, vol. 7, no. 2, pp. 868–878, 3 2016.

[20] Australian Energy Market Operator (AEMO), "Integrated System Plan For the National Electricity Market," 2022.